Since January 2020 Elsevier has created a COVID-19 resource centre with free information in English and Mandarin on the novel coronavirus COVID-19. The COVID-19 resource centre is hosted on Elsevier Connect, the company's public news and information website.

Journal of Molecular Liquids 340 (2021) 117224

Contents lists available at ScienceDirect

Journal of Molecular Liquids

journal homepage: www.elsevier.com/locate/molliq

Charge-transfer complexation of TCNE with azithromycin, the antibiotic used worldwide to treat the coronavirus disease (COVID-19). Part IV: A comparison between solid and liquid interactions

Abdel Majid A. Adam [a,*], Moamen S. Refat [a], Tariq A. Altalhi [a], Khaled Saleh Alsuhaibani [b]

[a] Department of Chemistry, College of Science, Taif University, P.O. Box 11099, Taif 21944, Saudi Arabia
[b] College of Pharmacy, King Saud University, Riyadh, Saudi Arabia

ARTICLE INFO

Article history:
Received 7 July 2021
Revised 3 August 2021
Accepted 8 August 2021
Available online 11 August 2021

Keywords:
Charge-transfer
Azithromycin
TCNE
Solid–solid interaction
Liquid–liquid interaction
Eco-friendly method

ABSTRACT

Finding a cure or vaccine for the coronavirus disease (COVID-19) is the most pressing issue facing the world in 2020 and 2021. One of the more promising current treatment protocols is based on the antibiotic azithromycin (AZM) alone or in combination with other drugs (e.g., chloroquine, hydroxychloroquine). We believe gaining new insight into the charge-transfer (CT) chemistry of this antibiotic will help researchers and physicians alike to improve these treatment protocols. Therefore, in this work, we examine the CT interaction between AZM (donor) and tetracyanoethylene (TCNE, acceptor) in either solid or liquid forms. We found that, for both phases of starting materials, AZM reacted strongly with TCNE to produce a colored, stable complex with 1:2 AZM to TCNE stoichiometry via a $n \rightarrow \pi^*$ transition (AZM → TCNE). Even though both methodologies yielded the same product, we recommend the solid–solid interaction since it is more straightforward, environmentally friendly, and cost- and time-effective.

1. Introduction

A charge transfer (CT) interaction, commonly referred to as a CT reaction or CT complexation, involves one molecule donating electrons to another molecule [1–8]. The former donor (D) molecule is electron-rich while the latter acceptor (A) molecule is electron-deficient. The chemistry of CT interactions has received considerable interest from researchers year after year because it yields new complexes with unique chemical and physical properties that render them beneficial to pharmacology, medicine, industry, and academia (biology, physics, biochemistry, and chemistry). Many synthesized CT complexes have high electrical conductivity/super conductivity and strong magnetism, and, therefore, contribute to many important electrical conductor, superconductor, optoelectronic, light-emitting, and solar energy storage devices [9–23]. Moreover, countless synthesized CT complexes exhibit promising antitumor, anti-inflammatory, and antimicrobial properties. CT interactions are used to study and understand biological processes in the human body (e.g., DNA binding, enzymatic reactions) and the thermodynamics and pharmacodynamics of therapeutic compounds (e.g., mechanism of action, drug delivery) [24–32]. Every year, considerable research efforts are dedicated to producing new CT complexes, investigating their properties (e.g., photophysical, thermodynamic, crystallographic, spectral, kinetic), and determining which factors affect the CT interactions (e.g., type of solvent, time, concentration, temperature) [18,33–53].

Azithromycin (AZM; $C_{38}H_{72}N_2O_{12}$, 748.98 g/mol; Fig. 1) is an orally bioactive, highly effective, well-tolerated, broad-spectrum antibiotic used to treat infectious diseases caused by both Gram-positive and Gram-negative bacteria. In addition to its antibacterial properties, AZM also has antimalarial, anti-inflammatory, immunomodulatory, and antiviral effects [54–57]. AZM caught the world's attention in 2020 because it showed promising results in the treatment of severe acute respiratory syndrome coronavirus 2 (SARS-CoV-2) disease, commonly known as COVID-19. This syndrome was first identified in Wuhan, China on December 9, 2019, and spread swiftly throughout China and around the globe [58]. By early March 2020, the World Health Organization (WHO) declared the COVID-19 outbreak a pandemic [59]. At that point, the global rush began to find means to conquer this pandemic and stop its psychological, medical, and economic burdens [60]. AZM has been incorporated into the treatment protocols for COVID-19 alone and in conjugation with other drugs (e.g., chloroquine, hydroxychloroquine). This protocol is clinically effective and now widely used around the world as a short-term course [61–66].

We believe providing new insight into the CT chemistry of AZM will help researchers and physicians alike to improve the treat-

* Corresponding author.
E-mail address: majidadam@tu.edu.sa (A.M.A. Adam).

https://doi.org/10.1016/j.molliq.2021.117224
0167-7322/

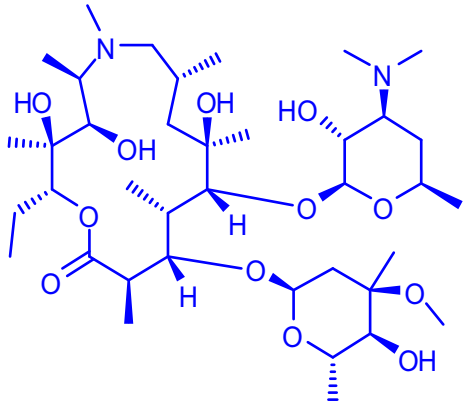

Fig. 1. Structure of the AZM molecule.

ment protocols for COVID-19. As a continuation of our previous works [67–69] that aim to furnish a big-picture perspective on the CT chemistry of azithromycin by examining its complexation with several acceptors (σ- and π-) and the resultant CTCs, in this work, we examine the CT interaction between AZM (donor) and tetracyanoethylene (TCNE; acceptor) in both the solid–solid and liquid–liquid states. The solid–solid interaction generated a solid CT complex by grinding solid AZM and TCNE powders together without adding any solvents, while the liquid–liquid interaction also resulted in a solid CT complex but by mixing acetonitrile solutions of AZM and TCNE and filtering off the formed precipitate.

2. Materials and methods

2.1. Materials

The AZM powder ($C_{38}H_{72}N_2O_{12}$; 748.98 g/mol; purity ≥ 98%), tetracyanoethylene (TCNE) (C_6N_4; 128.1 g/mol; purity 96%), and acetonitrile (CH_3CN; 41.05 g/mol; purity 99.8%) were all analytical grade, procured from the Sigma-Aldrich Chemical Company (USA) at the highest purity available, and used as received. AZM and TCNE were completely dissolved in CH_3CN solvent.

2.2. Characterization methods

The UV–visible absorption spectra and the FT-IR spectra were scanned using a DR6000 Benchtop HACH LANGE UV/VIS Spectrophotometer (200–800 nm) and IR Tracer-100 Shimadzu Fourier-Transform Infrared Spectrophotometer, respectively. The nitrogen, hydrogen, and carbon composition (in percentages) were determined using a PE 2400 Series II Perkin-Elmer CHN Microanalyzer.

2.3. Synthetic methods

2.3.1. Product 1

Product 1 was generated by grinding solid AZM and TCNE powders together without adding any solvent [35,70–72]. Specifically, 0.749 g of AZM (1 mmol) and 0.256 g of TCNE (2 mmol) were put in a dry, clean porcelain mortar. Then, the two components were ground together thoroughly using a pestle for 5 min until a uniform, solid powder was generated. Finally, the obtained yellow homogenate, termed *Product 1*, was collected and stored in a vacuum desiccator with $CaCl_2$ (anhydrous) at room temperature to protect it from humidity. FT-IR and elemental analyses were used to characterize the product. IR data: 3485 and 3251 ν(O—H), 2974 $\nu_{asym}(CH_3)$, 2938 $\nu_{asym}(CH_2)$, 2890 $\nu_{sym}(CH_3)$, 2830 $\nu_{sym}(CH_2)$, 2200 and 2262 ν(C≡N) 1718 ν_{asym}(C═O), 1595 ν_{sym}(C═O), 1500 ν(C═C), 1461 $\delta_{rock}(CH_3)$, 1374 $\delta_{scissor}(CH_2)$, 1276 $\delta_{rock}(CH_2)$, 1165 ν_{asym}(C—N), 1080 ν_{sym}(C—N), 1041 ν(C—O), 995 ν(C—C), 900 δ(O—H) in-plane bending, 800 $\delta_{wag}(CH_3)$, 731 ν(O—H) out-of-plane bending, and 558 $\delta_{twist}(CH_2)$. Elemental data (%): yellow powder; $C_{44}H_{72}N_6O_{12}$ (877.1 g mol^{-1}); observed (calculated) for N, 9.35 (9.58); H, 8.42 (8.21); C, 59.92 (60.20).

2.3.2. Product 2

Product 2 was generated by mixing acetonitrile solutions of AZM and TCNE and filtering off the formed precipitate [73–76]. Specifically, solutions of AZM (1 mmol in 20 mL CH_3CN) and TCNE (2 mmol in 20 mL CH_2CN) were mixed thoroughly using a magnetic stirrer for 15 min at room temperature. The volume of the mixture was reduced by half using a water bath, then left for 24 h at room temperature to ensure complete precipitation. The resultant yellow precipitate was filtered through Whatman 42 grade filter paper, washed thoroughly using CH_3CN solvent, and then dried in a vacuum desiccator with $CaCl_2$ (anhydrous) at room temperature for 48 h. The resultant product was termed *Product 2* and characterized using FT-IR and elemental analyses. IR data: 3442 and 3227 ν(O—H), 2973 $\nu_{asym}(CH_3)$, 2933 $\nu_{asym}(CH_2)$, 2885 $\nu_{sym}(CH_3)$, 2830 $\nu_{sym}(CH_2)$, 2198 and 2163 ν(C≡N) 1721 ν_{asym}(C═O), 1594 ν_{sym}(C═O), 1500 ν(C═C), 1462 $\delta_{rock}(CH_3)$, 1380 $\delta_{scissor}(CH_2)$, 1263 $\delta_{rock}(CH_2)$, 1165 ν_{asym}(C—N), 1092 ν_{sym}(C—N), 1000 ν(C—O), 950 ν(C—C), 890 δ(O—H) in-plane bending, 803 $\delta_{wag}(CH_3)$, 720 ν(O—H) out-of-plane bending, and 620 $\delta_{twist}(CH_2)$. Elemental data (%): yellow powder; $C_{44}H_{72}N_6O_{12}$ (877.1 g mol^{-1}); observed (calculated) for N, 9.77 (9.58); H, 8.50 (8.21); C, 59.98 (60.20).

3. Results and discussion

3.1. CT absorption

The generation of a CT complex is typically associated with a strong color change upon combining the donor and acceptor. Therefore, UV–visible spectroscopy is the conventional technique used to detect such changes and to determine whether a CT interaction occurred and to characterize this interaction. The CT interaction alters the electronic absorption spectrum of the donor, acceptor, or both and this is reflected by the change in color. These spectral changes fall into two categories:

(i) Hypsochromic shifts: the appearance of a new absorption band in the UV–visible spectrum of the resultant CT complex where neither the free donor nor acceptor have any measurable absorption.
(ii) Bathochromic shifts: increases in intensity and/or size of the absorption band that characterized the donor, acceptor, or both.

In this work, upon mixing the solutions of AZM (10×10^{-3} M; colorless in CH_3CN solvent) and TCNE (10×10^{-3} M; pale brown in CH_3CN solvent), a strong color change was observed from pale brown to intense yellow color in the resultant CT complex, as pictured in Fig. 2. This type of color change is suggestive of a strong CT interaction between AZM and TCNE. Fig. 3 contains the UV–visible absorption of the AZM (5.0×10^{-4} M), TCNE (5.0×10^{-4} M), and the CT complex derived by mixing the two solutions (1:1). The solution of free AZM is CH_3CN solvent is colorless, with no measurable absorption bands in the UV–visible region. The solution of free TCNE in CH_3CN solvent was pale brown, with a broad absorption band ranging from 354 to 440 nm with a long tail ranging from 440 to 800 gradually decreasing in intensity. The broad band had two maximum heads at 395 and 414 nm. After TCNE complexed with AZM, the intensity of the broad band that characterized free

Fig. 2. Strong color change upon mixing TCNE (*far left*; *pale brown*) with AZM (*middle; colorless*) to produce the CT complex (*far right*; *intense yellow*) in the CH_3CN solvent.

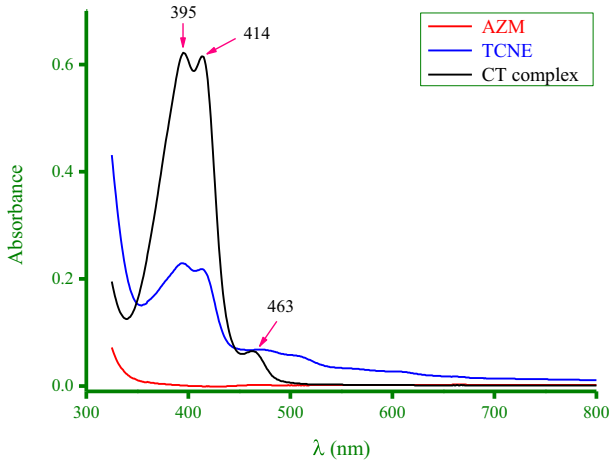

Fig. 3. UV–visible absorption spectra of the AZM (5.0×10^{-4} M), the TCNE (5.0×10^{-4} M), and their CT complex in CH_3CN solvent.

TCNE increased greatly and became a little much broader. These two heads were still present at the same positions but became clearer and sharper. The long tail was absent and, instead, a small weak band appeared at 463 nm. These spectral changes indicated bathochromic shifts occurred when AZM formed a CT complex with TCNE.

3.2. Product 1

Product 1 was generated through a solvent-free solid–solid interaction using a simple one-step method. Solid AZM (1 mmol) and TCNE (2 mmol) were ground together thoroughly in a porcelain mortar. AZM reacted with TCNE without any solvent to form a yellow-colored solid homogenate (*Product 1*), as pictured in Fig. 4. As shown in Fig. 4, solid AZM alone is white, solid TCNE alone is black, and grinding them together produced a yellow-colored product. This strong color change indicates that a CT complexation reaction occurred between the AZM and TCNE molecules through a solvent-free, solid–solid interaction. Fig. 5 shows the color of *Product 1* (yellow) and *Product 2* (yellow–brown). A sample of *Product 1* was elementally characterized. The obtained values for the N%, H%, and C% were 9.35%, 8.42%, and 59.92%, respectively. These data agree with the values calculated theoretically from the molecular formula of *Product 1* ($C_{44}H_{72}N_6O_{12}$; 877.1 g mol^{-1}), (calculated values 9.58%, 8.21%, and 60.20%, respectively). The elemental composition of *Product 1* confirmed that the solid–solid interaction between AZM and TCNE proceeded at a molar ratio of 1:2 (AZM to TCNE). A solution of *Product 1* was prepared in CH_3CN solvent at a concentration of 5.0×10^{-4} M and scanned by UV–visible spectroscopy; the resulting electronic absorption spectrum is presented in Fig. 6. The UV–visible absorption spectrum of *Product 1* was characterized by a very strong, broad band ranging from 345 to 480 nm with two maximum heads at 395 and 414 nm. A shoulder band was also detected at 463 nm. The shape of the UV–visible absorption spectrum of *Product 1* was similar to that of the CT complex produced by mixing solutions of AZM (5.0×10^{-4} M) and TCNE (5.0×10^{-4} M) (Fig. 3), confirming that the solvent-free, solid–solid approach produced a solid AZM-TCNE CT complex.

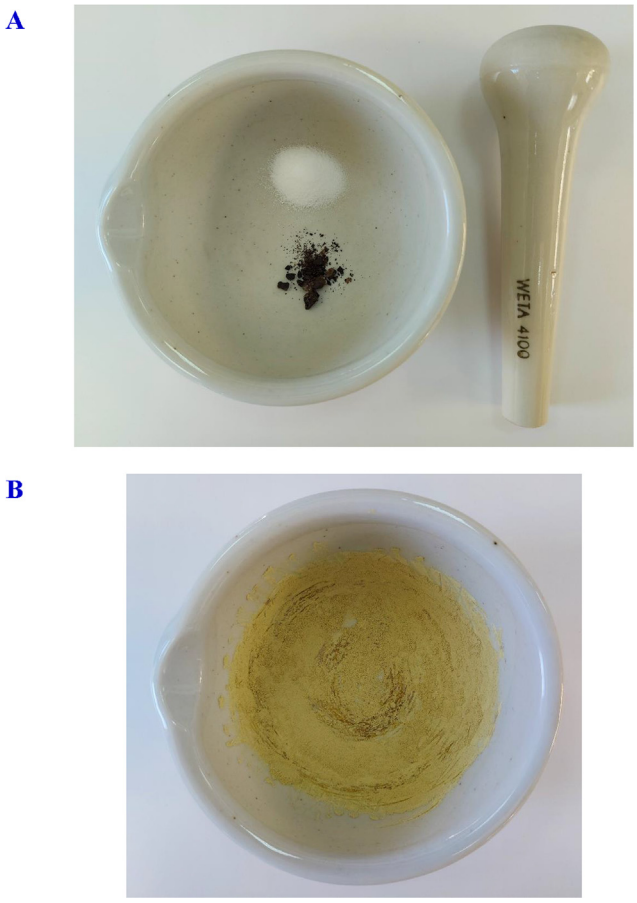

Fig. 4. Photograph of (A) AZM (up, white) and TCNE (down, black); (B) the resultant *Product 1* after grinding the two components for 5 min.

3.3. Product 2

Product 2 was generated from liquid-phase starting materials using a multi-step process involving a brief reaction period (~3 min), precipitate formation (~24 h), and product filtration and purification. As pictured in Fig. 5, this methodology resulted in a yellow–brown product. The elemental composition of *Product*

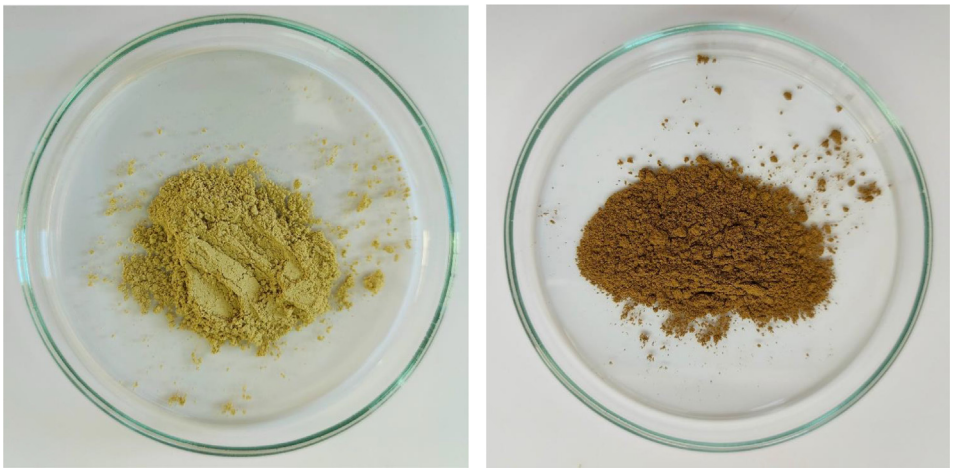

Fig. 5. Photograph of *Product 1* (left; yellow) and *Product 2* (right; yellowish-brown).

2 was N 9.77%, H 8.50%, and C 59.98%, which aligned with the theoretical values (N 9.58%, H 8.21%, C 60.20%) calculated from its molecular formula ($C_{44}H_{72}N_6O_{12}$; 877.1 g mol^{-1}). These results confirmed that the liquid–liquid interaction of AZM and TCNE proceeded via a 1:2 AZM to TCNE molar ratio, as did the solid–solid interaction. A solution of *Product 2* was prepared in CH_3CN solvent at 5.0×10^{-4} M to determine its electronic absorption spectrum. As shown in Fig. 6, the shape of the UV–visible absorption spectrum of *Product 2* is similar to that of the CT complex generated by mixing solutions of AZM (5.0×10^{-4} M) and TCNE (5.0×10^{-4} M) (Fig. 3). Both spectra contained a very strong, broad band ranging from 345 to 440 nm, with two maximum heads at 395 and 414 nm. A weak shoulder band was also detected at 463 nm. This confirmed that the liquid–liquid methodology produced a solid CT complex of AZM and TCNE. There were two differences in the UV–visible absorption spectra of the two products: *i)* in *Product 2*, the width of the band was less than that of *Product 1* by 40 nm; and *ii)* in *Product 2*, the intensity of the shoulder band at 463 nm was weaker than that of *Product 1*. These two differences in the electronic absorption spectra are reflected in the product's color (yellow *Product 1*, yellow–brown *Product 2)*.

3.4. IR measurements

Fig. 7 contains the FT-IR spectra of the free reactants (AZM and TCNE) and the FT-IR spectra of *Product 1* and *Product 2* are given in Fig. 8. The IR spectral data (in cm^{-1}) collected for the free AZM molecule were: 3490 and 3245 ν(O—H), 2971 $\nu_{asym}(CH_3)$, 2932 $\nu_{asym}(CH_2)$, 2883 $\nu_{sym}(CH_3)$, 2834 $\nu_{sym}(CH_2)$, 1719 ν_{asym}(C═O), 1660 ν_{sym}(C═O), 1465 $\delta_{rock}(CH_3)$, 1377 $\delta_{scissor}(CH_2)$, 1269 $\delta_{rock}(CH_2)$, 1181 ν_{asym}(C—N), 1083 ν_{sym}(C—N), 1040 ν(C—O), 992 ν(C—C), 895 δ(O—H) in-plane bending, 836 $\delta_{wag}(CH_3)$, 797 $\delta_{wag}(CH_2)$, 737 ν(O—H) out-of-plane bending, and 570 $\delta_{twist}(CH_2)$ (Fig. 7a). The AZM molecule contains five hydroxyl groups that produced three characteristic bands at 895, 737, and 3490–3245 cm^{-1} due to their in-plane bending, out-of-plane bending, and stretching vibrational modes. The AZM molecule contains 14 methyl groups (CH_3) that produced four characteristic bands at 2883, 2971, 1465, and 836 cm^{-1} due to the $\nu_{sym}(CH_3)$, $\nu_{asym}(CH_3)$, $\delta_{rock}(CH_3)$, and $\delta_{wag}(CH_3)$ modes, respectively. Also, the AZM molecule contains five methylene groups (CH_2). Their asymmetric and symmetric stretching vibrations gave bands at 2932 and 2834 cm^{-1},

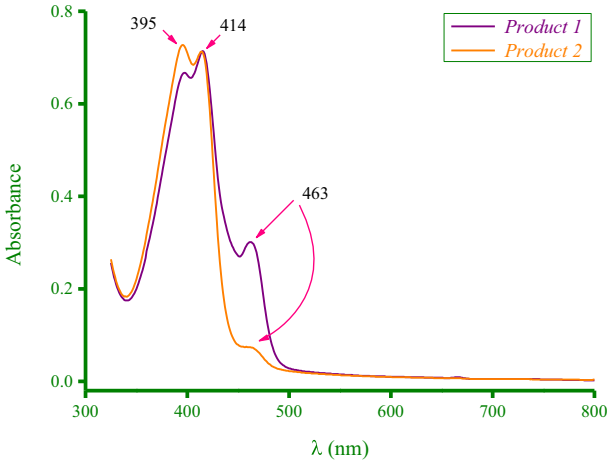

Fig. 6. UV–visible absorption spectra of *Product 1* and *Product 2* (5.0×10^{-4} M).

Fig. 7. (A). FT–IR spectrum of the free AZM molecule. (B). FT–IR spectrum of the free TCNE molecule.

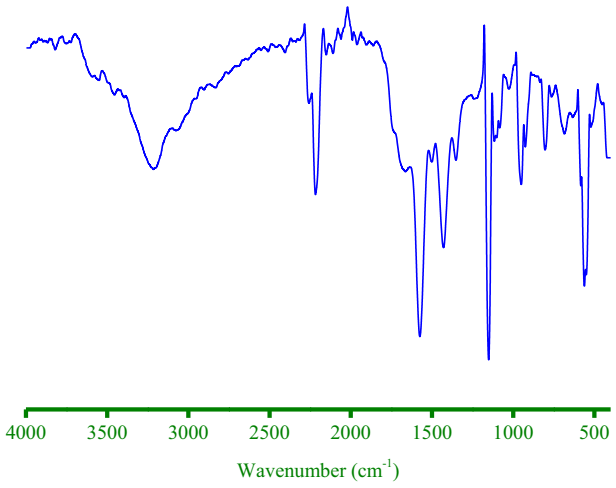

Fig. 7 (*continued*)

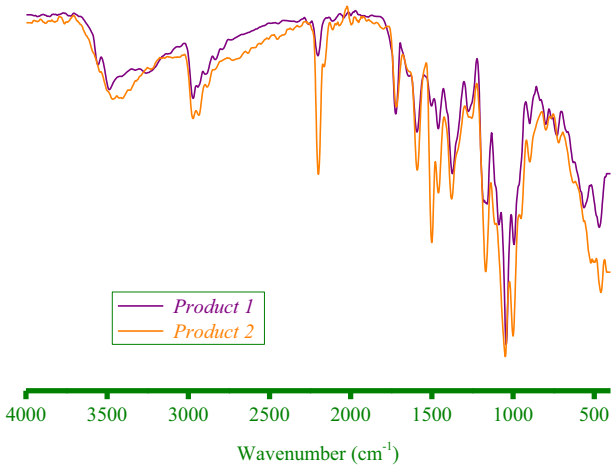

Fig. 8. FT–IR spectra of *Product 1* and *Product 2*.

respectively. Their bending vibrations, twisting, wagging, rocking, and scissoring, produced bands at 570, 797, 1269, and 1377 cm^{-1}, respectively. The very strong band resonating at 1040 cm^{-1} resulted from the ν(C—O) vibration. The sharp, medium-strong band at 1719 cm^{-1} was assigned to the ν_{asym}(C═O) vibrational mode, while the broad, weak band located at 1660 cm^{-1} was attributed to the ν_{sym}(C═O) mode. The IR spectrum of the free TCNE molecule (Fig. 7b) had absorption bands with wavenumbers 563, 684, 800, 952, 1152, 1575, (2219 and 2256), and 3217 cm^{-1} attributed to the vibrational motions of δ_{wag}(-C—C—C), $\delta_{scissor}$(C—C—C), δ_b(C—C—C), ν_{sym}(C—C), ν_{asym}(C—C), ν(C═C), ν(C≡N), and ν(O—H); H_2O, respectively [77]. The IR spectra of *Product 1* and *Product 2* (Fig. 8) contained all of the principal bands of the AZM and TCNE molecules, and, in general, the two products exhibited similar IR spectra. The ν(C═C) vibration of free TCNE resonated as a very strong band at 1575 cm^{-1}. After complexation with AZM, the intensity of this band decreased and shifted to a lower frequency (1500 cm^{-1} in both *Product 1* and *Product 2*). The displacement of the ν(C═C) vibration by about ~75 cm^{-1} suggests that the C═C moiety of the TCNE molecule participated in the CT bonding with AZM. The ν(C≡N) vibration of free TCNE conferred a medium-strong band at 2219 cm^{-1} with a shoulder band at 2256 cm^{-1}. After TCNE interacted with AZM, this band shifted to a lower frequency (2200 cm^{-1} in *Product 1*, 2198 cm^{-1} in *Product 2*). The absorption band observed at 1181 cm^{-1} from the ν_{asym}(C—N) vibration of free AZM shifted to 1165 cm^{-1} in both products after complexation with TCNE. This shift implicates nitrogen atoms in the CT bonding between AZM and TCNE. The changes to the ν(C═C) bands of free TCNE and ν_{asym}(C—N) bands of free AZM observed in their products (*Product 1* and *Product 2*) suggested that the charge transferred from the N-atoms in the AZM molecule to the C═C moiety of the TCNE molecule, which represents a direct $n \rightarrow \pi^*$ transition, as proposed in Fig. 9 [35,51,78–80].

3.5. Comparison between the methodologies

A colored, solid CT complex between the AZM and TCNE molecules was synthesized using two methodologies that differed by the phase of the starting materials (solid–solid vs liquid–liquid). The data collected in this study support that both methodologies successfully produced the intended AZM-TCNE CT complex through a direct $n \rightarrow \pi^*$ transition (AZM → TCNE). Generating this complex using the solid–solid approach is simpler and faster because it is a one-step process that, unlike the liquid–liquid approach, does not require solvents or a purification process. As such, the liquid–liquid methodology is more complex, costly, and time-consuming than its solid–solid counterpart. Table 1 contains a comparison of the two methodologies.

4. Conclusions

After the WHO declared the COVID-19 outbreak a pandemic, a global race began to stop its spread and the associated psychological, medical, and economic burden by finding a cure or vaccine for this disease. Several antibiotics have been tested, current treatment protocols for COVID-19 involve the antibiotic azithromycin (AZM) alone or in combination with other compounds. Giving a vision to the charge-transfer (CT) chemistry of AZM may help clinicians and researchers to improve the treatment protocols for COVID-19. Comparing the CT interactions between AZM donor and TCNE acceptor molecules achieved using two approaches (solid–solid and liquid–liquid) revealed that the former reacts strongly with the latter to produce a colored, stable complex regardless of whether the phase of the starting materials is solid or liquid. Under both conditions, the interaction between AZM and TCNE is a $n \rightarrow \pi^*$ transition (AZM → TCNE) that proceeds with 1:2 AZM to TCNE stoichiometry. The solid–solid approach is preferable over the liquid–liquid one because it is a simpler, faster means

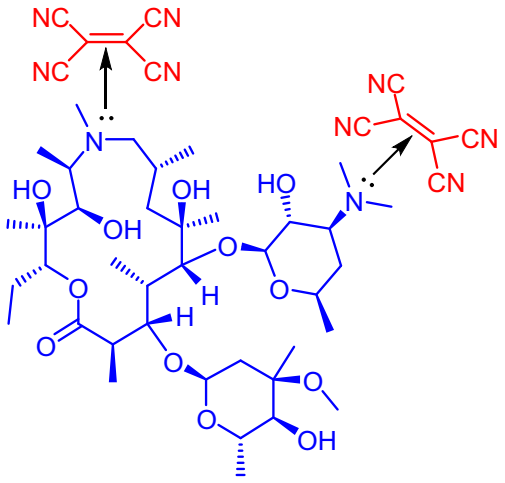

Fig. 9. Proposed chemical structure of *Product 1* and *Product 2*.

Table 1
Comparison between the solid–solid and liquid–liquid approaches to synthesizing an AZM-TCNE CT complex.

Parameter	Solid-solid interaction	Liquid-liquid interaction
Ease	Simple one-step process	Complex multi-step process
Speed	Rapid	Slow
Cost	Low	Higher
Additional reagents	No	Yes
Time	Short	Longer
Environmental impact	Eco-friendly	–Requires solvent –Generates liquid waste
Color	Yellow	Yellow-brown
UV spectrum	–Broad absorption band –Strong band at 463 nm	–Narrow absorption band –Weak band at 463 nm
IR spectrum	Similar	Similar
Interaction type	$n \rightarrow \pi^*$ transition	$n \rightarrow \pi^*$ transition
Produces the desired CT complex	Yes	Yes

of yielding the same product and, therefore, more time-efficient, cost-effective, and eco-friendly. Complexation between AZM and acceptor molecules can be achieved easily through solid–solid interaction and may improve the efficacy of this antibiotic against specific infections, such as that causing the COVID-19 pandemic.

CRediT authorship contribution statement

Abdel Majid A. Adam: Data curation, Funding acquisition, Investigation, Project administration, Supervision, Writing – original draft, Writing – review & editing. **Moamen S. Refat:** Data curation, Funding acquisition, Investigation, Project administration, Supervision, Writing – original draft, Writing – review & editing. **Tariq A. Altalhi:** Conceptualization, Formal analysis, Methodology, Resources, Software, Validation, Visualization. **Khaled Saleh Alsuhaibani:** Conceptualization, Formal analysis, Methodology, Resources, Software, Validation, Visualization.

Declaration of Competing Interest

The authors declare that they have no known competing financial interests or personal relationships that could have appeared to influence the work reported in this paper.

Acknowledgments

This work was supported by Taif University Researchers Supporting Project Number (TURSP-2020/02), Taif University, Taif, Saudi Arabia. The authors are very grateful to Dr. Leah Boyer (San Diego, CA, USA) for reviewing and editing the manuscript.

References

[1] S. Shakya, I.M. Khan, Charge transfer complexes: Emerging and promising colorimetric real-time chemosensors for hazardous materials, J. Hazard. Mater. 403 (2021) 123537.
[2] A.S. Al-Attas, M.M. Habeeb, D.S. Al-Raimi, Spectrophotometric determination of some amino heterocyclic donors through charge transfer complex formation with chloranilic acid in acetonitrile, J. Mol. Liq. 148 (2–3) (2009) 58–66.
[3] J. Seliger, V. Zagar, K. Gotoh, H. Ishida, A. Konnai, D. Amino, T. Asaji, Hydrogen bonding in 1,2-diazine–chloranilic acid (2 : 1) studied by a ^{14}N nuclear quadrupole coupling tensor and multi-temperature X-ray diffraction, PCCP 11 (13) (2009) 2281–2286.
[4] A.S. Gaballa, C. Wagner, S.M. Teleb, E.M. Nour, M.A.F. Elmosallamy, G.N. Kaluderovic, H. Schmidt, D. Steinborn, Preparation, spectroscopic and structural studies on charge-transfer complexes of 2,9-dimethyl-1,10-phenanthroline with some electron acceptors, J. Mol. Struct. 876 (1–3) (2008) 301–307.
[5] R.S. Mulliken, W.B. Person, Molecular Complexes, Wiley, New York, 1969.
[6] R.S. Mulliken, Structures of complexes formed by halogen molecules with aromatic and with oxygenated solvents, J. Am. Chem. Soc. 72 (1950) 600–608.
[7] R. Foster, Organic Charge-Transfer Complexes, Academic Press, London, 1969.
[8] R.S. Mulliken, Molecular compounds and their spectra. III. The interaction of electron donors and acceptors, J. Phys. Chem. 56 (7) (1952) 801–822.
[9] Y. Liang, W. Xing, L. Liu, Y. Sun, W. Xu, D. Zhu, Charge transport behaviors of a novel 2:1 charge transfer complex based on coronene and HAT$(CN)_6$, Org. Electron. 78 (2020) 105608.
[10] G.G. Parra, A.L.S. Pavanelli, L.P. Franco, L.N.C. Máximo, R.S. da Silva, I. Borissevitch, Interaction of CdTe-MPA quantum dots with meso-tetra methyl pyridyl porphyrin. Charge transfer complex formation, J. Photochem. Photobiol., A 398 (2020) 112580.
[11] J. Li, X. Zhang, J. Nie, X. Zhu, Visible light and water-soluble photoinitiating system based on the charge transfer complex for free radical photopolymerization, J. Photochem. Photobiol., A 402 (2020) 112803.
[12] A. El-Bindary, Z. Anwar, T. El-Shafaie, Effect of silicon dioxide nanoparticles on the assessment of quercetin flavonoid using Rhodamine B Isothiocyanate dye, J. Mol. Liq. 323 (2021) 114607.
[13] O.A. El-Gammal, F.S. Mohamed, G.N. Rezk, A.A. El-Bindary, Synthesis, characterization, catalytic, DNA binding and antibacterial activities of Co(II), Ni(II) and Cu(II) complexes with new Schiff base ligand, J. Mol. Liq. 326 (2021) 115223.
[14] S. Lee, J. Hong, S. Jung, K. Ku, G. Kwon, W.M. Seong, H. Kim, G. Yoon, I. Kang, K. Hong, H.W. Jang, K. Kang, Charge-transfer complexes for high-power organic rechargeable batteries, Energy Storage Mater. 20 (2019) 462–469.
[15] T. Salzillo, N. Crivillers, M. Mas-Torrent, K. Wurst, J. Veciana, Synthesis of a vinylogue tetrathiafulvalene derivative and study of its charge transfer complex with $TCNQF_4$, Synth. Met. 247 (2019) 144–150.
[16] X. Chen, H. Wang, B. Wang, Y. Wang, X. Jin, F. Bai, Charge transport properties in organic D-A mixed-stack complexes based on corannulene and sumanene derivatives-a theoretical study, Org. Electron. 68 (2019) 35–44.
[17] G. Kang, S. He, H. Cheng, X. Ren, Enhanced intramolecular charge transfer of organic dyes containing hydantoin donor: a DFT study, J. Photochem. Photobiol., A 383 (2019) 111979.
[18] L. Man, T. Li, X. Wu, K. Lu, L. Yang, X. Liu, Z. Yang, J. Zhou, C. Ni, Synthesis, crystal structure, vibrational spectra, nonlinear optical property of an organic charge-transfer compound-4-nitrobenzyl isoquinolinium picrate based on DFT calculations, J. Mol. Struct. 1175 (2019) 971–978.
[19] M.V. Rusalov, V.V. Volchkov, V.L. Ivanov, M.Y. Melnikov, F.E. Gostev, V.A. Nadtochenko, A.I. Vedernikov, S.P. Gromov, M.V. Alfimov, Ultrafast excited state dynamics of a stilbene–viologen charge transfer complex and its interaction with alkanediammonium salts, J. Photochem. Photobiol., A 372 (2019) 89–98.
[20] A.S.A. Almalki, A. Alhadhrami, A.M.A. Adam, I. Grabchev, M. Almeataq, J.Y. Al-Humaidi, T. Sharshar, M.S. Refat, Preparation of elastic polymer slices have the semiconductors properties for use in solar cells as a source of new and renewable energy, J. Photochem. Photobiol., A 361 (2018) 76–85.
[21] A.S.A. Almalki, A. Alhadhrami, R.J. Obaid, M.A. Alsharif, A.M.A. Adam, I. Grabchev, M.S. Refat, Preparation of some compounds and study their thermal stability for use in dye sensitized solar cells, J. Mol. Liq. 261 (2018) 565–582.
[22] A.M.A. Adam, M.S. Refat, H.A. Saad, Quick and simple formation of different nanosized charge-transfer complexes of the antibiotic drug moxifloxacin: an efficient way to remove and utilize discarded antibiotics, C.R. Chimie 18 (2015) 914–928.
[23] I.M. Khan, A. Ahmad, S. Kumar, Synthesis, spectroscopic characterization and structural investigations of a new charge transfer complex of 2,6-diaminopyridine with 3,5-dinitrobenzoic acid: DNA binding and antimicrobial studies, J. Mol. Struct. 1035 (2013) 38–45.
[24] I.M. Khan, M. Islam, S. Shakya, K. Alam, N. Alam, M. Shahid, Synthesis, characterization, antimicrobial and DNA binding properties of an organic charge transfer complex obtained from pyrazole and chloranilic acid, Bioorganic Chem. 99 (2020) 103779.
[25] I.M. Khan, S. Shakya, R. Akhtar, K. Alam, M. Islam, N. Alam, Exploring interaction dynamics of designed organic cocrystal charge transfer complex of 2-hydroxypyridine and oxalic acid with human serum albumin: single crystal, spectrophotometric, theoretical and antimicrobial studies, Bioorganic Chem. 100 (2020) 103872.
[26] S. Niranjani, K. Venkatachalam, Synthesis, spectroscopic, thermal, structural investigations and biological activity studies of charge-transfer complexes of atorvastatin calcium with dihydroxy-*p*-benzoquinone, quinalizarin and picric acid, J. Mol. Struct. 1219 (2020) 128564.
[27] A. Karmakar, P. Bandyopadhyay, S. Banerjee, N.C. Mandal, B. Singh, Synthesis, spectroscopic, theoretical and antimicrobial studies on molecular charge-transfer complex of 4-(2-thiazolylazo)resorcinol (TAR) with 3, 5-dinitrosalicylic acid, picric acid, and chloranilic acid, J. Mol. Liq. 299 (2020) 112217.
[28] R. Kavitha, S. Nirmala, R. Nithyabalaji, R. Sribalan, Biological evaluation, molecular docking and DFT studies of charge transfer complexes of quinaldic acid with heterocyclic carboxylic acid, J. Mol. Struct. 1204 (2020) 127508.
[29] M.E. Mohamed, E.Y.Z. Frag, A.A. Hathoot, E.A. Shalaby, Spectrophotometric determination of fenoprofen calcium drug in pure and pharmaceutical preparations. Spectroscopic characterization of the charge transfer solid complexes, Spectrochim. Acta A 189 (2018) 357–365.

[30] O.R. Shehab, H. AlRabiah, H.A. Abdel-Aziz, G.A.E. Mostafa, Charge-transfer complexes of cefpodoxime proxetil with chloranilic acid and 2,3-dichloro-5,6-dicyano-1,4-benzoquinone: experimental and theoretical studies, J. Mol. Liq. 257 (2018) 42–51.
[31] G.G. Mohamed, M.M. Hamed, N.G. Zaki, M.M. Abdou, M.E. Mohamed, A.M. Abdallah, Melatonin charge transfer complex with 2,3-dichloro-5,6-dicyano-1,4-benzoquinone: molecular structure, DFT studies, thermal analyses, evaluation of biological activity and utility for determination of melatonin in pure and dosage forms, Spectrochim. Acta A 182 (2017) 143–159.
[32] N. Rahman, S. Sameen, M. Kashif, Spectroscopic study of charge transfer complexation between doxepin and π–acceptors and its application in quantitative analysis, J. Mol. Liq. 222 (2016) 944–952.
[33] C. Balraj, S. Balaji, M. Karthikeyan, Systematic measurements of charge transfer complexes caused from 1-phenyl-1,2,3,4-tetrahydroisoquinoline and 4-aminoacetanilide with series of π-acceptors (BQ, DDQ, TCNQ), Spectrochim. Acta A 245 (2021) 118931.
[34] I.M. Khan, K. Alam, M.J. Alam, Exploring charge transfer dynamics and photocatalytic behavior of designed donor-acceptor complex: characterization, spectrophotometric and theoretical studies (DFT/TD-DFT), J. Mol. Liq. 310 (2020) 113213.
[35] T.A. Altalhi, Utilization of tannic acid into spherical structured carbons based on charge-transfer complexation with tetracyanoethylene acceptor: liquid-liquid and solid-solid interactions, J. Mol. Liq. 300 (2020) 112325.
[36] M.T. Basha, R.M. Alghanmi, S.M. Soliman, W.J. Alharby, Synthesis, spectroscopic, thermal, structural characterization and DFT/TD-DFT computational studies for charge transfer complexes of 2,4-diamino pyrimidine with some benzoquinone acceptors, J. Mol. Liq. 309 (2020) 113210.
[37] P.S. Koroteev, A.B. Ilyukhin, K.A. Babeshkin, N.N. Efimov, Charge transfer complexes of lanthanide 3,5-dinitrobenzoates and 1,2-phenylenediamine, J. Mol. Struct. 1207 (2020) 127800.
[38] A. El-Dissouky, T.E. Khalil, H.A. Elbadawy, D.S. El-Sayed, A.A. Attia, S. Foro, X-ray crystal structure, spectroscopic and DFT computational studies of H-bonded charge transfer complexes of tris (hydroxymethyl)aminomethane (THAM) with chloranilic acid (CLA), J. Mol. Struct. 1200 (2020) 127066.
[39] O.A. El-Gammal, F.S. Mohamed, G.N. Rezk, A.A. El-Bindary, Structural characterization and biological activity of a new metal complexes based of Schiff base, J. Mol. Liq. 330 (2021) 115522.
[40] F.A. Al-Saif, A.A. El-Habeeb, M.S. Refat, H.H. Eldaroti, M.A. Abdel, H. Adam, H.A. S.a. Fetooh, Chemical and physical properties of the charge transfer complexes of domperidone antiemetic agent with π-acceptors, J. Mol. Liq. 293 (2019) 111517.
[41] F.A. Al-Saif, A.A. El-Habeeb, M.S. Refat, M.A. Abdel, H.A. Adam, A.I. Saad, H.F. El-Shenawy, Characterization of charge transfer products obtained from the reaction of the sedative-hypnotic drug barbital with chloranilic acid, chloranil, TCNQ and DBQ organic acceptors, J. Mol. Liq. 287 (2019) 110981.
[42] N. Venkatesh, B. Naveen, A. Venugopal, G. Suresh, V. Mahipal, P. Manojkumar, T. Parthasarathy, Donor-acceptor complex of 1-benzoylpiperazine with *p*-chloranil: synthesis, spectroscopic, thermodynamic and computational DFT gas phase/PCM analysis, J. Mol. Struct. 1196 (2019) 462–477.
[43] U. Neupane, M. Singh, P. Pandey, R.N. Rai, Synthesis, spectroscopic, crystal structure, thermal and optical studies of a novel proton transfer complex: 2-Methyl-8-hydroxyquinoliniumpicrate, J. Mol. Struct. 1195 (2019) 131–139.
[44] W. Falek, R. Benali-Cherif, L. Golea, S. Samai, N. Benali-Cherif, E. Bendeif, I. Daoud, A structural comparative study of charge transfer compounds: synthesis, crystal structure, IR, Raman-spectroscopy, DFT computation and hirshfeld surface analysis, J. Mol. Struct. 1192 (2019) 132–144.
[45] M. Faizan, Z. Afroz, M.J. Alam, V.H. Rodrigues, S. Ahmed, A. Ahmad, Structural, vibrational and electronic absorption characteristics of the monohydrate organic salt of 2-amino-5-bromo-6-methyl-4-pyrimidinol and 2,3-pyrazinedicarboxylic acid: a combined experimental and computational study, J. Mol. Struct. 1177 (2019) 229–241.
[46] K.S. Fathima, M. Sathiyendran, K. Anitha, Structure elucidation, biological evaluation and molecular docking studies of 3-aminoquinolinium 2-carboxy benzoate- A proton transferred molecular complex, J. Mol. Struct. 1176 (2019) 238–248.
[47] S. Soltani, P. Magri, M. Rogalski, M. Kadri, Charge-transfer complexes of hypoglycemic sulfonamide with π-acceptors: experimental and DFT-TDDFT studies, J. Mol. Struct. 1175 (2019) 105–116.
[48] A.A. El-Bindary, S.M. El-Marsafy, A.A. El-Maddah, Enhancement of the photocatalytic activity of ZnO nanoparticles by silver doping for the degradation of AY99 contaminants, J. Mol. Struct. 1191 (2019) 76–84.
[49] I.M. Khan, S. Shakya, N. Singh, Preparation, single-crystal investigation and spectrophotometric studies of proton transfer complex of 2,6-diaminopyridine with oxalic acid in various polar solvents, J. Mol. Liq. 250 (2018) 150–161.
[50] A.S.A. Almalki, A.M. Naglah, M.S. Refat, M.S. Hegab, A.M.A. Adam, M.A. Al-Omar, Liquid and solid-state study of antioxidant quercetin donor and TCNE acceptor interaction: Focusing on solvent affect on the morphological properties, J. Mol. Liq. 233 (2017) 292–302.
[51] A.M.A. Adam, M.S. Refat, M.S. Hegab, H.A. Saad, Spectrophotometric and thermodynamic studies on the 1:1 charge transfer interaction of several clinically important drugs with tetracyanoethylene in solution-state: part one, J. Mol. Liq. 224 (2016) 311–321.
[52] A.M.A. Adam, M.S. Refat, Solution and solid-state investigations of charge transfer complexes caused by the interaction of bathophenanthroline with different organic acceptors in a (methanol + dichloromethane) binary solvent system, J. Mol. Liq. 219 (2016) 377–389.
[53] A.M.A. Adam, M.S. Refat, H.A. Saad, M.S. Hegab, Charge transfer complexation of the anticholinergic drug clidinium bromide and picric acid in different polar solvents: solvent effect on the spectroscopic and structural morphology properties of the product, J. Mol. Liq. 216 (2016) 192–208.
[54] A. Firth, P. Prathapan, Azithromycin: The first broad-spectrum therapeutic, Eur. J. Med. Chem. 207 (2020) 112739.
[55] P. Zarogoulidis, N. Papanas, I. Kioumis, E. Chatzaki, E. Maltezos, K. Zarogoulidis, Macrolides: from in vitro anti-inflammatory and immunomodulatory properties to clinical practice in respiratory diseases, Eur. J. Clin. Pharmacol. 68 (5) (2012) 479–503.
[56] J. Min, Y.J. Jang, Macrolide therapy in respiratory viral infections, Mediators Infamm. 2012 (2012) 649570.
[57] I. Grgičević, I. Mikulandra, M. Bukvić, M. Banjanac, V. Radovanović, I. Habinovec, B. Bertoša, P. Novak, Discovery of macrozones, new antimicrobial thiosemicarbazone-based azithromycin conjugates: design, synthesis and in vitro biological evaluation, Int. J. Antimicrob. Agents 56 (5) (2020) 106147.
[58] N. Zhu, D. Zhang, W. Wang, X. Li, B. Yang, J. Song, X. Zhao, B. Huang, W. Shi, R. Lu, P. Niu, F. Zhan, X. Ma, D. Wang, W. Xu, G. Wu, G.F. Gao, D. Phil, W. Tan, A novel coronavirus from patients with pneumonia in China, 2019, N. Engl. J. Med. 382 (2020) 727–733.
[59] Organization WH. WHO director-General's opening remarks at the media briefing on COVID-19, 11 March 2020, Geneva, Switzerland; 2020.
[60] I. Ali, O.M.L. Alharbi, COVID-19: disease, management, treatment, and social impact, Sci. Total Environ. 728 (2020) 138861.
[61] N. Bakhshaliyev, M. Uluganyan, A. Enhos, E. Karacop, R. Ozdemir, The effect of 5-day course of hydroxychloroquine and azithromycin combination on QT interval in non-ICU COVID19(+) patients, J. Electrocardiol. 62 (2020) 59–64.
[62] P. Gautret, J. Lagier, P. Parola, V.T. Hoang, L. Meddeb, M. Mailhe, B. Doudier, J. Courjon, V. Giordanengo, V.E. Vieira, H.T. Dupont, S. Honoré, P. Colson, E. Chabrière, B. La Scola, J. Rolain, P. Brouqui, D. Raoult, Hydroxychloroquine and azithromycin as a treatment of COVID-19: results of an open-label non-randomized clinical trial, Int. J. Antimicrob. Agents 56 (1) (2020) 105949.
[63] A. Pain, M. Lauriola, A. Romandini, F. Scaglione, Macrolides and viral infections: focus on azithromycin in COVID-19 pathology, Int. J. Antimicrob. Agents 56 (2) (2020) 106053.
[64] S.M. Vouri, T.N. Thai, A.G. Winterstein, An evaluation of co-use of chloroquine or hydroxychloroquine plus azithromycin on cardiac outcomes: a pharmacoepidemiological study to inform use during the COVID19 pandemic, Res. Social. Adm. Pharm. (2020), https://doi.org/10.1016/j.sapharm.2020.04.031 [in press].
[65] R.L. Mitra, S.A. Greenstein, L.M. Epstein, An algorithm for managing QT prolongation in coronavirus disease 2019 (COVID-19) patients treated with either chloroquine or hydroxychloroquine in conjunction with azithromycin: possible benefits of intravenous lidocaine, HeartRhythm Case Rep. 6 (5) (2020) 244–248.
[66] S. Arshad, P. Kilgore, Z.S. Chaudhry, G. Jacobsen, D.D. Wang, K. Huitsing, I. Brar, G.J. Alangaden, M.S. Ramesh, J.E. McKinnon, W. O'Neill, M. Zervos, Treatment with hydroxychloroquine, azithromycin, and combination in patients hospitalized with COVID-19, Int. J. Infect. Dis. 97 (2020) 396–403.
[67] A.M.A. Adam, H.A. Saad, A.M. Alsuhaibani, M.S. Refat, M.S. Hegab, Charge-transfer chemistry of azithromycin, the antibiotic used worldwide to treat the coronavirus disease (COVID-19). Part I: Complexation with iodine in different solvents, J. Mol. Liq. 325 (2021) 115187.
[68] A.M.A. Adam, H.A. Saad, A.M. Alsuhaibani, M.S. Refat, M.S. Hegab, Charge-transfer chemistry of azithromycin, the antibiotic used worldwide to treat the coronavirus disease (COVID-19). Part II: Complexation with several π-acceptors (PA, CLA, CHL), J. Mol. Liq. 325 (2021) 115121.
[69] A.M.A. Adam, H.A. Saad, A.M. Alsuhaibani, M.S. Refat, M.S. Hegab, Charge-transfer chemistry of azithromycin, the antibiotic used worldwide to treat the coronavirus disease (COVID-19). Part III: A green protocol for facile synthesis of complexes with TCNQ, DDQ, and TFQ acceptors, J. Mol. Liq. 335 (2021) 116250.
[70] K.R. Mahmoud, M.S. Refat, T. Sharshar, A.M.A. Adam, E.A. Manaaa, Synthesis of amino acid iodine charge transfer complexes *in situ* methanolic medium: chemical and physical investigations, J. Mol. Liq. 222 (2016) 1061.
[71] T. Tanno, T. Oohashi, Formation of a green-form TTF–CA charge transfer complex confirmed with terahertz transmission spectrum, Res. Phys. 5 (2015) 74–75.
[72] J. Nishizawa, T. Tanno, T. Oohashi, H. Watanabe, Y. Oyama, Observation of the solid-state formation of a TTF–CA complex by terahertz spectroscopy, Synth. Met. 158 (7) (2008) 278–282.
[73] A.M.A. Adam, Nano-structured complexes of reserpine and quinidine drugs with chloranilic acid based on intermolecular H-bond: spectral and surface morphology studies, Spectrochim. Acta A 127 (2014) 107–114.
[74] M.S. Refat, A.M.A. Adam, Structural, thermal, kinetic and pharmacology in vitro studies of H-bonded complexes formed between the sedative-hypnotic drug 5,5-diethylbarbituratic acid with various acceptors: liquid and solid characterization, J. Mol. Liq. 196 (2014) 142–152.
[75] A.M.A. Adam, M.S. Refat, H.A. Saad, Spectral, thermal, XRD and SEM studies of charge-transfer complexation of hexamethylenediamine and three types of acceptors: π-, σ- and vacant *orbital* acceptors that include quinol, picric acid, bromine, iodine, $SnCl_4$ and $ZnCl_2$ acceptors, J. Mol. Struct. 1051 (2013) 144–163.
[76] A.M.A. Adam, M.S. Refat, H.A. Saad, Utilization of charge-transfer complexation for the detection of carcinogenic substances in foods: Spectroscopic

characterization of ethyl carbamate with some traditional π-acceptors, J. Mol. Struct. 1037 (2013) 376–392.
[77] T. Takenaka, S. Tadokoro, N. Uyeda, Infrared absorption spectra of tetracyanoethylene adsorbed on evaporated alkali halides, Bull. Inst. Chem. Res. Kyoto Univ. 48 (6) (1970) 249–263. http://hdl.handle.net/2433/76349.
[78] A.M.A. Adam, H.H. Eldaroti, M.S. Hegab, M.S. Refat, J.Y. Al-Humaidi, H.A. Saad, Measurements and correlations in solution-state for charge transfer products caused from the 1:2 complexation of TCNE acceptor with several important drugs, Spectrochim. Acta A 211 (2019) 166–177.
[79] A.M.A. Adam, M.S. Refat, Chemistry of drug interactions: characterization of charge-transfer complexes of Guaifenesin with various acceptors using spectroscopic and thermal methods, J. Gen. Chem. 84 (9) (2014) 1847–1856.
[80] A.M.A. Adam, Synthesis, spectroscopic, thermal and antimicrobial investigations of charge-transfer complexes formed from the drug procaine hydrochloride with quinol, picric acid and TCNQ, J. Mol. Struct. 1030 (2012) 26–39.